New Phytologist

The Arabidopsis mitogen-activated protein kinase 6 is associated with γ-tubulin on microtubules, phosphorylates EB1c and maintains spindle orientation under nitrosative stress

Journal:	*New Phytologist*
Manuscript ID:	NPH-MS-2014-18958.R1
Manuscript Type:	MS - Regular Manuscript
Date Submitted by the Author:	n/a
Complete List of Authors:	Kohoutová, Lucie; Institute of Microbiology, AS CR, Laboratory of Functional Cytology Kourová, Hana; Institute of Microbiology, AS CR, Laboratory of Functional Cytology Nagy, Szilvia; Semmelweis University, Department of Medical Chemistry, Molecular Biology and Pathobiochemistry Volc, Jindřich; Institute of Microbiology, AS CR, Laboratory of Functional Cytology Halada, Petr; Institute of Microbiology, AS CR, Laboratory of Molecular Structure Mészáros, Tamás; Semmelweis University, Department of Medical Chemistry, Molecular Biology and Pathobiochemistry Meskiene, Irute; University of Vienna, Max F Perutz Laboratories Vienna Bogre, Laszlo; Royal Holloway, University of London, School of Biological Sciences; Binarova, Pavla; Institute of Microbiology ASCR, Laboratory of Functional Cytology
Key Words:	Arabidopsis, cell division, γ-tubulin, EB1c, microtubules, mitogen-activated protein kinase, MPK6, nitrosative stress

The Arabidopsis mitogen-activated protein kinase 6 is associated with γ-tubulin on microtubules, phosphorylates EB1c and maintains spindle orientation under nitrosative stress

Lucie Kohoutová[1], Hana Kourová[1], Szilvia K. Nagy[2], Jindřich Volc[1], Petr Halada[1], Tamás Mészáros[2,5], Irute Meskiene[3], László Bögre[4], and Pavla Binarová[1#]

[1] Institute of Microbiology AS CR, v. v. i., Vídeňská 1083, 142 20 Prague 4, Czech Republic
[2] Semmelweis University, Department of Medical Chemistry, Molecular Biology and Pathobiochemistry, Tűzoltó u. 37-47, H-1094 Budapest, Hungary
[3] Max F. Perutz Laboratories, University of Vienna, Vienna, Austria, and Institute of Biotechnology, University of Vilnius, Lithuania
[4] Royal Holloway, University of London, School of Biological Sciences, Egham, Surrey, TW20 0EX, United Kingdom
[5] Technical Analytical Research Group of HAS, Szent Gellért tér 4, H-1111 Budapest, Hungary

Author for correspondence[#]:
Pavla Binarová
Telephone: +420 296 442 130
e-mail: binarova@biomed.cas.cz

Word Counts
Main body of text: 6443/6500
Introduction: 827
Materials and Methods: 1458
Results: 2616
Discussion: 1438
Acknowledgements: 104
Black and white figures: 2 (Figures 1, 4)
Colour figures: 6 (Figures 2, 3, 5-8)
Tables: 0
Supporting information (Fig. S1-S5, Table S1, Methods S1)

Key words: *Arabidopsis*, cell division, γ-tubulin, EB1c, microtubules, mitogen-activated protein kinase, MPK6, nitrosative stress

Summary

•Stress-activated plant MAP kinase pathways play roles in growth adaptation to the environment by modulating cell division through cytoskeletal regulation, but the mechanisms are poorly understood.

•We performed protein interaction and phosphorylation experiments with cytoskeletal proteins, mass spectrometric identification of MPK6 complexes, and immunofluorescence analyses of the microtubular cytoskeleton of mitotic cells using wild type, *mpk6-2* mutant, and plants overexpressing the MAP kinase inactivating phosphatase, AP2C3.

•We showed that MPK6 interacted with γ-tubulin and co-sedimented with plant microtubules polymerized *in vitro*. It was the active form of MAPK that was enriched with microtubules and followed similar dynamics to γ-tubulin, moving from poles to midzone during the anaphase-to-telophase transition. We found a novel substrate for MPK6, the microtubule plus end protein, EB1c. The *mpk6-2* mutant was sensitive to NO_2-Tyr treatment with respect to mitotic abnormalities, and root cells overexpressing AP2C3 showed defects in chromosomal separation and spindle orientation.

•Our data suggest that the active form of MAPK interacts with γ-tubulin on specific subsets of mitotic microtubules during late mitosis. MPK6 phosphorylates EB1c, but not EB1a, and has roles to maintain regular planes of cell division under stress conditions.

(Word Count 188/200)

Introduction

Mitogen-activated protein kinase (MAPK) cascades provide universal signalling modules that enable physiological adaptations in response to a variety of stress conditions. MAPK signalling is also utilised to regulate development (Xu & Zhang, 2014). Both environmental and developmental inputs may impact on plant growth through the regulation of cell proliferation, differentiation, and cytoskeletal organisation (Sasabe & Machida, 2012). Pivotal targets of MAPKs are transcription factors, but there are also cytoskeletal proteins that these pathways regulate. In plants however, knowledge about MAPK substrates, and specifically on the phosphorylation of cytoskeletal proteins, is limited (Ellis, 2012).

One of the best studied mitotic MAPK signalling pathways is the so called PQR signalling cascade that is controlled by the NACK kinesin and targets MAP65 proteins through MPK4 to regulate cytokinesis (Calderini *et al.*, 1998; Nishihama *et al.*, 2001; Sasabe *et al.*, 2011). In accordance, cells in the *mpk4* mutant show aberrant cytokinesis in *Arabidopsis* (Kosetsu *et al.*, 2010; Beck *et al.*, 2011). Another pathway involves MPK3 and MPK6; single mutants of *mpk3* or *mpk6* have no major developmental phenotypes or cell division abnormalities, while the *mpk3mpk6* double mutant is embryo lethal (Wang *et al.*, 2007). Thus, MPK3 and MPK6 were suggested to have redundant and dose-dependent functions (Xu & Zhang, 2014). In accordance, MPK3 and MPK6 were shown to have overlapping substrate recognition (Popescu *et al.*, 2009; Ellis, 2012; Sorensson *et al.*, 2012), and to play multiple roles including photomorphogenesis (Sethi *et al.*, 2014), specification of cell fate during stomatal development (Wang *et al.*, 2007), regulation of cell proliferation and differentiation in anthers and ovules (Hord *et al.*, 2008; Wang *et al.*, 2008), and regulation of cell proliferation during inflorescence development (Meng *et al.*, 2012). While MPK3 and MPK6 have redundant roles in some processes, they are not interchangeable in others (Wang *et al.*, 2008; Meng *et al.*, 2012). In one of the pathways, MPK6 is part of the YDA and MKK4/MKK5 MAPK signalling downstream of the ERECTA receptor kinases to regulate meristematic development and cell proliferation (Meng *et al.*, 2012). The YDA pathway, through MPK6, also targets MAP65 to regulate cortical microtubules and cytokinesis (Smekalova *et al.*, 2014).

Stress signals are frequently transmitted through the generation of reactive oxygen species (ROS) and MPK6 provides a pivotal signalling route by targeting nitrate reductase 2 to generate NO, which impacts on growth adaptation e.g. root development in *Arabidopsis* (Wang *et al.*, 2010). Modification of tyrosinated α-tubulin by nitration affects microtubular dynamics and its association with MAPs (Blume *et al.*, 2013). However, whether the regulatory function of MPK6 in NO signalling plays a role in root development by targeting the microtubular cytoskeleton is not known.

MAPK signalling is intricately connected with the cytoskeleton, either directly through the phosphorylation of cytoskeletal proteins, or via interactions with cytoskeletal scaffolding proteins that may bring MAPKs together with their activators, substrates, or components of other pathways (Meister *et al.*, 2013). There are numerous examples in animal and yeast cells for interactions of MAP kinases with microtubular proteins in response to stress or developmental cues. For example MAP kinases regulate microtubular dynamics

during osmotic stress in yeast cells (Hagan, 2008). The role for MAPKs in microtubule assembly and capture on kinetochores was suggested in pig oocytes (Sun *et al.*, 2001). Active ERK kinases were necessary for normal spindle and metaphase plate formation, and for γ-tubulin localisation on spindle poles during maturation of mouse oocytes (Lee *et al.*, 2007). Signalling through ERK is involved in regulating the function of microtubule plus end protein EB1, where an interaction of STIM1 with EB1 is regulated through ERK phosphorylation (Pozo-Guisado *et al.*, 2013).

Despite extensive studies of plant MAPKs and their role in development, only a few substrates have been identified among microtubular proteins (Komis *et al.*, 2011; Sasabe & Machida, 2012). The microtubule-associated proteins, MAP65-1, MAP65-2, and MAP65-3, are the only ones that were experimentally shown to be regulated by MAPK signalling in mitotic plant cells. Phosphorylation of MAP65-1 by MAP kinase in tobacco (*Nicotiana tabacum*) regulates phragmoplast expansion through microtubule destabilization (Sasabe *et al.*, 2006). *Arabidopsis* MAP65-1 is phosphorylated both by MPK4 and by MPK6 *in vitro* (Smertenko *et al.*, 2006). MAP65-2 and MAP65-3 were also shown to be phosphorylated by MPK4 (Kosetsu *et al.*, 2010; Sasabe *et al.*, 2011). MAP65-1 and MAP65-2 have redundant functions in *Arabidopsis* with MAP65-3 in cytokinesis (Sasabe *et al.*, 2011).

Our biochemical data and cellular analyses of mitotic events show that MPK6 interacts with γ-tubulin and the microtubule plus end protein EB1c. The active form of MAPK is specifically recruited to kinetochore microtubular fibres of the mitotic spindle, and later, to midzone microtubules facing the chromatin, where it localizes together with γ-tubulin. We show that EB1c, but not EB1a, is phosphorylated by MPK6. The analysis of mitosis and cytokinesis in root meristematic cells with overexpression of AP2C3 MAPK phosphatase and the *mpk6* mutant uncovered a role for the regulation of chromosomal separation and spindle orientation, and links MPK6 to such functions by NO_2-Tyr treatment.

Materials and Methods

Plant material and cultured cells

Cell suspension cultures of *Arabidopsis thaliana* ecotype Landsberg erecta (Ler) and EB1c-GFP and Columbia (Col) were grown under continuous darkness at 25 °C as described previously (Drykova *et al.*, 2003). Seedlings of *Arabidopsis thaliana* (L.) Heynh. ecotype

Columbia, *mpk6-2* (Liu & Zhang, 2004), and AP2C3 oe (Umbrasaite *et al.*, 2010) were grown on half-strength Murashige-Skoog medium (Duchefa Biochemie, Haarlem, Netherlands) supplemented with 0.25 mM MES, pH 5.7, 1% (w/v) agar and 0.5 % sucrose under 16 h of light and 8 h of dark. C-terminal GFP fusion of EB1c was prepared by Gateway cloning using pDONR207 and pK7FWG2 destination vector (Karimi *et al.*, 2002). The construct was transformed to cell culture Ler through *Agrobacterium tumefaciens* GV3101 strain.

Immunopurification, gel permeation chromatography, electrophoresis and Western blotting

Protein extracts from *Arabidopsis* cultured cells were prepared as described before (Tomastikova *et al.*, 2012). For seedlings, 25 mM Tris pH 7.5, 75 mM NaCl, 15 mM EGTA, 10 mM $MgCl_2$, 0.1% Tween 20 with the same inhibitors as for cultures was used. Protein samples were solubilized for at least 1h with 1% Nonidet P-40 (Roche Diagnostics).

Immunopurifications were performed from solubilized protein extracts (~ 3 mg ml^{-1}). Extracts were incubated with primary antibody at 4°C, then Protein A-Agarose beads (Roche Diagnostics) were added and incubated for another 2 hours. After washing with 0.1% Nonidet P-40 in extraction buffer, and 50 mM Tris pH 8.0 with 150 mM NaCl, and finally without salt, elution was done either by 0.1% immunogenic peptide at room temperature or the beads were boiled with Laemmli buffer. Eluates were concentrated on Microcon Ultracel YM-30 (Millipore, Darmstadt, Germany); for proteomics, eluates were pooled from four experiments. Immunopurifications using GFP-TrapA (ChromoTek, Planegg-Martinsried, Germany) were performed according to the manufacturer's instructions. Lambda protein phosphatase (NEB, P0753) treatment was performed on EB1c-GFP bound on the beads for 40 min at 30°C according to manufacturer's instructions. Protein samples were separated on 8%, 10%, or 12% SDS-PAGE and transferred to 0.45 μm polyvinylidene fluoride membrane (Immobilon-P, Millipore) or nitrocelulose membrane (Whatman, GE Healthcare) by wet electroblotting and immunodetected with appropriate antibodies. SuperSignal West Pico Chemiluminiscent Substrate (Thermo Scientific, Rockford, Illinois, USA) or ECL Prime Western Blotting System (GE Healthcare) was used according to manufacturer's instructions. At least three independent experiments were performed; representative Western blots are shown.

Custom polyclonal rabbit antibody against MPK6 (GenScript) was raised against the C-terminal sequence LIYREALAFNPEYQQ (aa 381-395) of MPK6 molecule and affinity-purified on immunogenic peptide, custom polyclonal rabbit antibody AthTU against γ-tubulin

was raised as described in Drykova et al. (2003). Antibodies for immunodetection were used in the following dilutions: anti-AtMPK6 (Sigma) 1:4,000, p-ERK antibody against phosphorylated forms of MPKs Phospho-p44/42 MAPK (Erk1/2) (Thr202/Tyr204) (D13.14.4E) XP (Cell Signaling) 1:2,000, antibody 4B9 (kindly provided by Dr. R. J. Ferl) 1:2,400, anti-MAP65-1 (kindly provided by Prof. P. Hussey) 1:2,000, anti-EB1 (ab50187, Abcam) 1:2,000, DM1A (Sigma) 1:1,000, anti-GCP4 (custom polyclonal rabbit antibody affinity-purified on immunogenic peptide (GenScript) 1:200, anti-GFP (Abcam) 1:4,000, anti-γ-tubulin AthTU 1:3,000, anti-phospho-Thr (9381, Cell Signaling) 1:1,000. Secondary horseradish peroxidase conjugated antibodies; anti-mouse and anti-rabbit were diluted 1:7,500 and 1:10,000, respectively (Promega, Madison, USA; Cell Signaling, Danvers, MA, USA; Jackson ImmunoResearch Laboratories, Suffolk, UK).

The microtubule spin-down experiments were performed as described previously (Drykova *et al.*, 2003). For immunopurifications from microtubular pellets obtained by spin-downs, the pellets were resuspended and microtubules were depolymerized on ice in buffer containing Ca^{2+}.

Protein digestion and LC MALDI-TOF mass spectrometry were performed as described in Tomastikova et al., 2012 with slight modifications. For details see Methods S1.

Plasmid construction, *in vitro* transcription and *in vitro* translation

Coding regions of MPK6, γ-tubulin, EB1c, EB1a, and GCP4 were amplified from cDNA library by PCR and transferred into pEU3-NII-HLICNot and pEU3-NII-GLICNot vectors by ligation independent cloning. myc-AtMKK4-GOF was inserted into pEU3-NII-gateway vector by gateway cloning (Nagy & Meszaros, 2014). Plasmids purified from ampicillin-resistant colony were sequenced to confirm the PCR accuracy.

The *in vitro* mRNA synthesis was accomplished by addition of 1 µg of purified, NotI linearized vector according to the manufacturer's instructions (TrascriptAid T7 High Yield Transcription Kit, Thermo Scientific). The reaction was incubated for 2h at 37°C, precipitated by ammonium acetate/ethanol mixture, dissolved in 1x SUB-AMIX and stored at -80 °C. Quality and quantity of mRNAs was verified on agarose gel electrophoresis. Cell-free translation was carried out in 20.6 µl final volume by addition of 5 µL (15 µg) mRNA, 10 µL WEPRO® (Cell Free Sciences, Matsuyama, Japan) solution, 0.8 µL creatine kinase (1 mg ml^{-}

[1]) and 5 µL 1x SUB-AMIX. Additional 0.5 µl of myc-AtMKK4GOF mRNA was added to the translation mixture where His6-AtMPK6 was to be activated. The translation solution was underlayed to 206 µL SUB-AMIX in a sterile 96-well plate and the reaction was incubated for 20 hours at 20°C (Nagy & Meszaros, 2014).

Protein purification, phosphatase treatment, TEV protease cleavage

In vitro translated His6-AtMPK6 proteins were purified by affinity chromatography on 10 µl TALON® Magnetic Beads (Clontech, Mountain View, CA, USA). 50 mM sodium phosphate buffer complemented with 10 mM imidazole, 300 mM NaCl, 0.1% Triton-X was used as wash and binding buffer. The resin was washed three times after 1h incubation with total translation mixture at room temperature. TEV protease was affinity purified after bacterial protein expression using pTH24_TEV construct (van den Berg *et al.*, 2006). TEV protease cleavage was performed overnight and at 4 °C with addition of 2.5 µl 20X TEV Buffer (1 M Tris-HCl, pH 8.0, 10 mM EDTA), 0.5 µl 0.1 M DTT, 10 µl TEV protease to affinity purified proteins. *In vitro* translated GST-γ-tubulin, GST-GCP4, GST-EB1a and, GST-EB1c were purified by affinity chromatography on 25 µl Glutathione Magnetic Beads (Thermo Scientific). 125 mM Tris, 150 mM NaCl, pH 8.0 was used as wash and binding buffer. Phosphatase treatment was carried out with λ Protein Phosphatase (New England Biolabs, Hitchin, UK) for 30 minutes at 30°C.

In vitro kinase assays

For kinase assays 300 and 100 ng *in vitro* translated, affinity purified substrate and kinase was used, respectively. The assay was carried out in 20 mM Hepes, pH 7.5, 100 µM ATP, 1 mM DTT, 15 mM $MgCl_2$, 5 mM EGTA, 5 µCi [γ-32P]ATP with bead bound GST-γ-tubulin, GST-GCP4, GST-EB1a, and GST-AtEB1c as substrates in 16 µl final volume for 1 hour at room temperature, then stopped by addition of 5× Laemmli SDS buffer. Samples were fractionated on a 10% SDS-PAGE gel. The gel was fixed, stained with Coomassie Blue, dried and analysed by autoradiography.

Drug treatments

APM (amiprophos-methyl, Duchefa Biochemie A0185) or taxol (Paclitaxel, Sigma T7402) were diluted in DMSO and used in working concentrations of 10 μM for 2 h. Stock solution of 20 mM U0126 (Sigma U120) in DMSO was applied to Murashige-Skoog medium for cultured cells (pH 7.0) to working concentration of 20 μM. Cells were pretreated by 20 μM U0126 in thin layer in dark without shaking for 2 h; then transferred to fresh medium with 20 μM U0126 and shaken at 120 rpm for 30 – 40 min before collecting; then they were immediately frozen in liquid nitrogen and processed for biochemistry or for immunofluorescence. Mock treatment was done with DMSO. Working concentration of 0.5 μM NO_2-Tyr (3-nitro-L-tyrosine, Sigma N7389) in 0.5 μM HCl were used in half strenght Murashige-Skoog medium; 0.5 μM HCl was used for the mock treatment.

Microscopy

Immunofluorescence labelling was performed as described earlier (Drykova *et al.*, 2003). Whole-mounts were performed according to Sauer *et al.* (Sauer *et al.*, 2006). Dilution of antibodies: anti-AtMPK6 (Sigma) 1:1,000-1:2,000, p-ERK (Cell Signaling) 1:500, DM1A (Sigma) 1:2,000, anti-γ-tubulin TU-32 antibody (kindly provided by Dr. P. Dráber, IMG AS CR, Prague) (1:6), anti-AtMPK3 (Sigma) 1:1,000, anti-AtMPK4 (Sigma) 1:2,000, anti-GFP (Roche Diagnostics) 1:1,000, anti-KNOLLE (Rose Biotechnology-Secant Chemicals, Winchendon, MA, USA) 1:6,000, anti-γ-tubulin AthTU 1:2,000, phospho-Histone H3 (Ser10) (Cell Signaling) 1:200. Alexa Fluor 488, Alexa Fluor 594, DyLight 647-conjugated anti-mouse and anti-rabbit antibodies (Jackson ImmunoResearch Laboratories) were diluted 1:600, 1:800, 1:700, respectively. Chromatin was stained by DAPI.

For fluorescence microscopy Olympus IX-81 FV-1000 confocal imaging system with oil immersion objectives 100x/1.45 and 60x/1.35 was used; DAPI ex 405 nm, em 425-460 nm; Alexa488 ex 473 nm, em 485-545 nm; Alexa 594 ex 559 nm, em 575-640 nm; Alexa 647 ex 635 nm, em 655-755 nm. Laser scanning was performed using the sequential multitrack mode to avoid bleed-through. Images were analysed by FV10 ASW2.0 (Olympus, Tokyo, Japan) and prepared in Adobe Photoshop CS4 and Adobe Illustrator CS4 (adobe Systems). For macroscopic images magnifying microscope Leica MZ16F with DFC 320R2 camera and DFC Twain 7.5.0 SW (Leica, Wetzlar, Germany) was used. At least three independent experiments were performed; representative images are shown.

Multiple sequence alignment was done using ClustalW2 (Larkin *et al.*, 2007).

Accession numbers: MPK6 At2g43790, TubG1 At3G61650, EB1A At3g47690, EB1C At5g67270, GCP4 At3g53760, AP2C3 At2g40180

Results

MPK6 is associated with γ-tubulin on microtubules in proliferating cells

To investigate MPK6 protein complexes, we performed immunopurification from extracts of *Arabidopsis* cultured cells in exponential growth phase using anti-MPK6 antibody, and specifically eluted MPK6 complexes using the immunogenic peptide. As a control we used pre-immune serum. We identified proteins by LC-MALDI-TOF mass spectrometry (Table S1). We reproducibly identified γ-tubulin among the proteins in the MPK6 immunoprecipitate, but not in the negative control with pre-immune serum. The association of MPK6 with γ-tubulin was validated on Western blots (Fig. 1a). To confirm the interaction of γ-tubulin with MPK6, we performed reciprocal immunopurification experiments. Using a peptide-purified plant specific γ-tubulin antibody, we found that MPK6 was associated with immunopurified γ-tubulin from extracts of *Arabidopsis* cultured cells (Fig. 1b).

To investigate whether MPK6 was associated with γ-tubulin on microtubules, we polymerized plant microtubules with taxol from extracts of cultured cells and performed spin down assays that we have previously established to show association of γ-tubulin with microtubules (Drykova *et al.*, 2003). The S70 high speed supernatant of a soluble cytoplasmic extract was used for taxol-driven polymerization of microtubules (Fig. 1c). α-Tubulin, together with microtubule associated protein, MAP65-1, as well as the microtubule plus end proteins EB1s, were detected in microtubular pellets but these proteins were undetectable in the negative control where taxol was omitted. As we published earlier (Drykova *et al.*, 2003), γ-tubulin is pelleted with taxol-polymerized plant microtubules, and in accordance, γ-tubulin complex protein GCP4 was also detected in the microtubular fraction (Fig. 1c). The presence of microtubular nucleator proteins γ-tubulin and GCP4, plus end proteins EB1s, and microtubule-associated protein MAP65-1 collectively show efficient polymerization of plant microtubules *in vitro*.

The same microtubular fractions were used to test the association of MPK6 with plant microtubules. As shown in Fig. 1c, a portion of the soluble pool of MPK6 sedimented with taxol-polymerized microtubules. To determine whether active MAPKs were present with microtubules, we used a commercially available antibody directed against active phosphorylated ERK1 (p-ERK) that was shown to recognize the conserved phospho-epitope on the activation loop of plant MAPKs (Umbrasaite *et al.*, 2010). We found a large enrichment of phosphorylated MAPKs in microtubular pellets (Fig. 1c).

To determine whether the microtubule bound γ-tubulin or γ-tubulin complexes interacted with MPK6, we released the γ-tubulin complex by depolymerization of pelleted microtubules and performed immunopurification with peptide-purified antibody against plant γ-tubulin. As shown in Fig. 1d, MPK6 was detected with γ-tubulin immunoprecipitated from the microtubular fraction. We conclude that the active MAPK form is specifically enriched with *in vitro* polymerized plant microtubules and that MPK6 associates with microtubule-bound γ-tubulin.

MPK6 kinase was localised on mitotic microtubules in root meristematic cells

To gain further insights into the association of MPK6 with microtubules within mitotic cells, we analysed the localisation of MPK6 and p-ERK in *Arabidopsis* root meristems. Double immunofluorescence labelling showed that the signal for MPK6 was present in the area of the pre-prophase band (PPB; Fig. 2a, arrows), with the metaphase spindle (Fig. 2a, arrowheads), and with the phragmoplast (Fig. 2a, asterisk). The signal for p-ERK was not observed with PPBs (Fig. 2b, arrows), but was present with the spindle (Fig. 2b, arrowhead) and phragmoplast (Fig. 2b, asterisk). In anaphase, MPK6 localised with shortening kinetochore microtubular fibres (Fig. 2c, arrowheads) and was present in the midzone of the anaphase spindle (Fig. 2c, arrow). In contrast, p-ERK labelling was largely associated with shortening kinetochore microtubular fibres on the poles of the anaphase spindle (Fig. 2d, arrowheads). These immunolocalisation data suggested that the active form of MAPK was associated with specific subsets of mitotic microtubules. To test the correspondence of p-ERK signal and MPK6, we performed Western blotting with wild type Col-0 and *mpk6-2* mutant seedlings. We found that a significant portion of p-ERK detected-MAPK corresponds to MPK6 (Fig. S1a). To determine whether MPK6 labelling on mitotic microtubules was specific, we localised two other abundant MAPKs (Fig. S1b). We found that the immunofluorescence

signal for MPK3 was largely diffuse while the MPK4 signal was detected mainly in the midzone of the anaphase spindle, as was found previously (Beck *et al.*, 2011).

To ascertain whether MPK6 and p-ERK were associated with microtubules, we treated cells with the microtubule stabilizing drug, taxol, and the depolymerization drug, amiprophos methyl (APM). Both MPK6 and p-ERK signals were enriched in dense microtubular arrays of taxol-treated cells (Fig. S2a,b) and became dispersed in the cytoplasm when microtubules were depolymerized by APM (Fig. S2c). As shown in Figs. S2c and d, the signal for p-ERK was enriched in the vicinity of persistent kinetochore microtubular stubs that were abundantly decorated with γ-tubulin (Binarova *et al.*, 2000).

p-ERK is dynamically co-localised with γ-tubulin on kinetochore fibres and in the midzone during the anaphase-to-telophase transition

In animal cells, γ-tubulin is predominantly a centrosomal protein, while, as we described previously (Drykova *et al.*, 2003), it associates in cell cycle-specific patterns with mitotic microtubules in acentrosomal plant cells. Because MPK6 was immunopurified with γ-tubulin and p-ERK labelling showed similar labelling patterns to γ-tubulin on microtubules, we performed double immunofluorescence analyses of MPK6 and p-ERK with γ-tubulin in mitotic cells of *Arabidopsis* roots. As shown in Fig. 2e-g, the signal for p-ERK was present, together with the signal for γ-tubulin, on shortening polar kinetochore microtubular fibres during anaphase and with the phragmoplast in telophase. To analyse the co-localisation of MPK6 and p-ERK with γ-tubulin, we inspected mitotic figures in more detail and derived intensity profiles during anaphase-to-telophase transition. γ-Tubulin predominantly localised with shortening kinetochore fibres on poles of the anaphase spindle, and became gradually more abundant in the vicinity of separated chromatin facing the midzone, where phragmoplast microtubules were known to be nucleated (Binarova *et al.*, 2000). p-ERK followed the γ-tubulin signal with some delay, which was substantiated by the intensity profiles (Fig. 3a-d). In contrast to p-ERK that co-localised with γ-tubulin on kinetochore microtubules of the anaphase spindle, and with early phragmoplast microtubules, the signal for MPK6 was more pronounced in the entire midzone during anaphase and cytokinesis (Fig. 3e,f).

Because of the close association of γ-tubulin with MPK6 and p-ERK, we set out to test whether γ-tubulin can be phosphorylated by MPK6. γ-Tubulin was translated *in vitro* and an *in vitro* kinase assay was carried out with MKK4-activated MPK6. As shown in Fig. 4a, under

the conditions used, we could not detect γ-tubulin phosphorylation by active MPK6. This finding suggested that proteins of γ-tubulin complexes might be potential substrates for MAP kinase signalling. A database search indicated AtGCP4 to be a plausible candidate for MAP kinase phosphorylation, with a docking motif for MAPKs as well as a MAPK phosphorylation site at its N-terminus (http://elm.eu.org). We cloned and translated *in vitro* GCP4 protein and performed an *in vitro* kinase assay with activated MPK6. Similarly to γ-tubulin, phosphorylation of GCP4 protein could not be detected (Fig. 4a).

Altogether our data suggest that the active form of MAPK, recognised by p-ERK antibody, specifically enriched with plant microtubules polymerized *in vitro*, co-localised in cells with γ-tubulin on shortening anaphase kinetochore fibres on poles of the acentrosomal spindle and with a specific subset of phragmoplast microtubules in the vicinity of chromatin during phragmoplast formation. MPK6 is recruited to γ-tubulin or γ-tubulin complexes, but we could not find direct phosphorylation of either γ-tubulin or γ-tubulin complex protein GCP4 with MPK6 *in vitro*.

MPK6 interacts with and phosphorylates microtubule plus end protein EB1c but not EB1a

Microtubule plus ends proteins, the EB1s, were associated with microtubules polymerized from cell extracts of *Arabidopsis* (Fig. 1c). Furthermore, we found that MPK6 interacted with EB1 proteins immunopurified with anti-EB1 antibody that recognised multiple EB1 family members (Fig. 4b). To test whether plant EB1proteins were substrates for MPK6, we translated *in vitro* EB1a and EB1c and carried out a protein kinase assay with activated MPK6. We found that EB1a, similarly to γ-tubulin and GCP4, was not phosphorylated, while EB1c protein was phosphorylated by MPK6 under the same *in vitro* kinase assay conditions (Fig. 4a). The EB1c is a plant specific subtype of EB1 proteins with distinct nuclear localisation and the knock out mutants showed strong cell division defects (Komaki *et al.*, 2010). EB1c but not EB1a and EB1b has predicted MAP kinase phosphorylation sites and docking motif on C-terminal of the molecule (http://elm.eu.org, http://gps.biocuckoo.org), Fig. S3. We used cells expressing EB1c-GFP as an input for GFP immunopurification and confirmed that MPK6 interacted with EB1c (Fig. 4c). Reciprocally, we could also show that immunoprecipitation with MPK6 led to EB1c-GFP as well as the endogenous EB1c co-immunoprecipitation (Fig. 4d). We found that the immunoprecipitated EB1c-GFP was

phosphorylated on threonine based on the detection with phospho-threonine (p-Thr) antibody. The p-Thr signal was specific as it became diminished by Lamda protein phosphatase treatment (Fig. 4f). Additionally, when the activity of MAP kinases was inhibited by treatment of cells with a selective MEK inhibitor, U0126 (Fig. 4e), we found that the signal for phospho-threonine on EB1c was reduced (Fig.4f).

We also followed p-ERK and MPK6 localisation with EB1c-GFP protein using double immunolocalisation. In interphase, EB1c-GFP was localized in nuclei, similarly to MPK6, and p-ERK antibody recognized MAP kinases. The EB1c-GFP signal and the signal for the p-ERK decorated metaphase spindle were detected with slight accumulation in the vicinity of the kinetochores, as substantiated by intensity profiles (Fig. 5a). In anaphase, p-ERK and EB1c-GFP co-localised on shortening kinetochore fibres (Fig. 5b). In early telophase, when p-ERK labelling was present mainly on newly formed phragmoplast microtubules adjacent to separated chromatin, EB1c-GFP was localised prominently on the midline of the phragmoplast (Fig. 5c). MPK6 localised with EB1c-GFP in the spindle area (Fig. 5d), and a diffuse MPK6 signal was observed in the midzone during late anaphase and telophase (Fig. 5e,f).

Our data suggest that EB1c co-localises with the active form of MAPK at specific mitotic stages and that EB1c, but not EB1a, is directly phosphorylated by MPK6.

MPK6 is required for regulation of the alignment of cell division upon NO_2-Tyr treatment

Reactive oxygen species (ROS) are known to induce rapid activation of MPK6 that activates nitrate reductase 2 (NIA2), leading to increased nitric oxide (NO) production (Wang *et al.*, 2010). The product of NO signalling, nitrated tyrosine N-Tyr, is incorporated into α-tubulin in mammals and plants and disrupts the tyrosination/detyrosination cycle of microtubules required for the regular association and functions of MAPs and molecular motors (Blume *et al.*, 2013). To investigate the connection between NO and MPK6 functions in the regulation of mitotic microtubule organisation, we treated WT and *mpk6-2* mutant seedlings with NO_2-Tyr as an exogenous source of N-Tyr. We found that treatment of wild type Col-0 seedlings with NO_2-Tyr resulted in shortened roots and reduced mitotic activity in the cell division zone, as previously demonstrated (Lipka & Muller, 2014). As shown in Fig. 6a, the *mpk6-2* mutant was more sensitive to NO_2-Tyr treatment. Immunofluorescence analyses of whole

mount α-tubulin-labelled roots showed that the number of mitotic figures (MF) was more reduced upon long term treatment with 0.5 μM NO_2-Tyr in *mpk6-2* mutants (10 MF per root, SD = 2.7, n = 24) compared to Col-0 plants (16 MF per root, SD = 7.1, n = 24) (Fig. S4). Roots grown under NO_2-Tyr treatment showed the alignment of spindles to become oblique in wild type Col-0 (Fig. 6c), which is in agreement with published data (Lipka & Muller, 2014). While we could not detect mitotic abnormalities in *mpk6-2* mutant plants grown under control conditions (Fig. 6d), the effect of NO_2-Tyr on spindle and phragmoplast alignment was enhanced in the *mpk6-2* mutant compared to the WT plants (Fig. 6e, Fig. S4). Misaligned spindles and phragmoplasts (9.7 % for Col-0, n = 390 and 15.2 % for *mpk6-2* mutant, n = 230), disturbed cell files and enlarged cells were all indicative of defects in microtubulal organization and cell division. Altogether these data showed that the effects of NO_2-Tyr on the microtubular cytoskeleton, cell plane alignment and cell division were more pronounced in the *mpk6-2* mutant background.

Inactivation of MAPKs through the overexpression of AP2C3 phosphatase resulted in mitotic abnormalities in chromosomal separation and spindle alignment

Overexpression of AP2C3 phosphatase (At2g40180) preferentially inhibits *Arabidopsis* MAPKs MPK3, MPK4, and MPK6 and these seedlings show largely disturbed root development (Fig. 7) as well as cell division defects in the stomatal lineage (Umbrasaite *et al.*, 2010). We looked for cell division defects in the roots of AP2C3 oe plants. Instead of regular cell files typical for the meristematic and transition zones of the WT roots, cell files of AP2C3 oe roots were disrupted, and cells were of various sizes and shapes, often isodiametric and swollen (Fig. 7a). Closer inspection revealed mitotic defects in AP2C3 oe. Chromosomes were not congressed in the metaphase plate (54.4 %, n = 136, $p < 0.01$) (Fig. 7b,f), and lagging chromosomes were observed in anaphase (58.2 %, n = 55, $p < 0.01$) (Fig. 7c, arrowhead, f). Chromosomes remained condensed and formed round-shaped masses in the cells that failed to enter telophase (8.4 %, n = 274, $p < 0.01$) (Fig. 7c, arrow, f). Microtubules, instead of being organised in spindles or phragmoplasts, were randomly arranged in the vicinity of chromatin, and labelling of cytokinetic syntaxin, KNOLLE, revealed complete failure of cell plate formation. Nuclei were often enlarged or lobed (Fig. 7c, asterisk). Both spindles (14.7 %, n = 191, $p < 0.01$) (Fig. 7d, arrow, f) and phragmoplasts (20.1 %, n = 274, $p < 0.01$) were misaligned in AP2C3 oe roots (Fig. 7e, arrows, f).

As an alternative approach to reduce MAP kinase activity, we used the selective MEK inhibitor, U0126. Treatment of *Arabidopsis* cells with U0126 reduced phosphorylation of MAP kinases, as detected by p-ERK antibody on Western blot (Fig. 4e, 8a). S70 extracts from U0126 treated cells were used as an input for taxol-driven polymerization of plant microtubules; the spin down assays were performed in the presence of the inhibitor. As shown in Fig. 8a, the p-ERK signal detected with samples of sedimented microtubules was severely reduced in comparison to untreated controls. On the other hand, the detected MAP65-1 signal in microtubular pellets from extracts of U0126 treated cells was stronger (Fig. 8a). This data suggest that the majority of MAP65-1 was bound to microtubules under conditions of reduced MAP kinase activity. Levels of γ-tubulin and EB1 proteins in microtubular pellets did not differ dramatically in U0126 treated samples (Fig. 8a).

We then performed immunofluorescence labelling to analyse microtubular mitotic arrays and cell division in cells where activity of MAP kinases was reduced due to U0126 treatment. Instead of the regular metaphase and anaphase mitotic figures, as shown in Fig. 2, we observed defects of congression of mitotic chromosomes and chromosomal separation defects. Despite abundant microtubules in microtubular kinetochore fibres of long mitotic spindles (Fig. 8b, arrows), chromosomes were unattached and free in the cytoplasm (Fig. 8c, arrowheads). γ-Tubulin accumulated on poles (Fig. 8b) and in the vicinity of unattached chromosomes (Fig. 8c). Spindles were elongated and astral microtubules were observed on poles of acentrosomal anaphase spindles, which failed to separate chromosomes (Fig. 8e). Aberrant phragmoplasts with bundled microtubules were present when separated chromatin was already decondensed (Fig 8d, arrow and arrowheads). The γ-tubulin signal with aberrant phragmoplasts was weak and did not show a gradient on phragmoplast microtubules from chromatin to the midzone, as typically found in control anaphase cells (Fig. 3), and accumulated around the nuclei (Fig. 8d). An aberrant telophase with unattached chromosomes negative for mitotic phospho-histone H3 labelling was observed (Fig. 8f).

Altogether these data suggest that inactivation of several MAPKs through the overexpression of the MAPK phosphatase AP2C3 abrogates chromosomal separation and cytokinesis. Similar mitotic defects were observed in cells where MAP kinase activity was inhibited by treatment with the specific MEK inhibitor, U0126.

Discussion

Plant cells are surrounded by a rigid cell wall yet their division in plant meristems is plastic and is continuously tuned by developmental signals and environmental conditions. In acentrosomal plant cells, this is achieved by the flexible assembly, dynamic regulation and interchange of plant-specific mitotic and cytokinetic arrays. How developmental and environmental signals influence the dynamics of plant microtubules, either directly through phosphorylation of microtubules or through phosphorylation of microtubule-associated proteins, is still not well understood. The best studied signalling pathways that respond to developmental and stress signals, and regulate microtubules, are the MAPK pathways, but the identification of cytoskeletal phosphorylated targets in plant cells is so far limited to MAP65-1, MAP65-2, and MAP65-3 (Sasabe *et al.*, 2006; Kosetsu *et al.*, 2010; Sasabe *et al.*, 2011). Our *in vitro* and *in situ* data showed that MPK6 is present on microtubules, and the active MAP kinase associates with a specific subset of mitotic and cytokinetic microtubules. In seeking proteins associated with MPK6, by purification of MPK6 protein complexes and mass spectrometric analysis of associated proteins, we identified γ-tubulin, a highly conserved eukaryotic protein with functions in microtubular nucleation as well as with non-canonical functions in the cell cycle and in nuclear processes (Horejsi *et al.*, 2012). We showed that kinetochore-localised γ-tubulin is important for plant spindle organisation (Binarova *et al.*, 2000), and later kinetochore functions of γ-tubulin were also confirmed in animal cells (Mishra *et al.*, 2010). Our finding that MPK6 associates with γ-tubulin was not completely unexpected. For example, mitotic defects observed in mouse oocytes, when p38 MAPK was depleted, indicated that MAPKs are important components of the microtubular organizing centre (Ou *et al.*, 2010). Inhibition of MAP kinase activity reduced the recruitment of γ-tubulin to centrosomes and nucleation activity of the centrosomes (Colello *et al.*, 2012).

We demonstrated that MPK6 is associated with γ-tubulin; however, it remains unclear whether this is a direct interaction. We could not find evidence that MPK6 phosphorylates γ-tubulin *in vitro* and similarly we did not show phosphorylation for GCP4, a member of the γ-tubulin complex GCP proteins. Although we cannot exclude that MPK6 might regulate other GCPs or another γ-tubulin interacting proteins, our data suggest that a scaffolding role for γ-tubulin might exist in MPK6 signalling to microtubules.

γ-Tubulin, in coordination with microtubule plus end proteins or with molecular motors, was shown to function in organisation of the microtubular cytoskeleton during mitosis (Bouissou *et al.*, 2014; Olmsted *et al.*, 2014) and its role in scaffolding of proteins of microtubule plus ends was suggested (Cuschieri *et al.*, 2006). We found that MPK6 not only interacts with γ-

tubulin, but also with EB1 proteins. EB1a and the highly similar EB1b form a subgroup of plant EB1 proteins with conserved roles of tracking plus ends of microtubules, while EB1c is a plant-specific EB1 protein with nuclear localization and strong cell division phenotypes in mutant (Komaki *et al.*, 2010). We found that only EB1c but not EB1a was phosphorylated by MPK6, suggesting that MPK6 through EB1c regulates mitotic division in response to external signals. To learn more about functions of EB1c, we searched for co-expressed genes in available databases (Toufighi *et al.*, 2005). EB1c shows significant co-expression with checkpoint proteins, MAD2 and BUB3. These findings correspond well with the cellular localisation of EB1c on kinetochore fibres and at cytokinetic sites, suggesting functions for EB1c in the regulation of cell division (Van Damme *et al.*, 2004). Mutant analyses indeed showed roles for EB1c in spindle positioning, chromosomal congression and segregation (Komaki *et al.*, 2010). Some of the cell division defects in EB1c mutants are reminiscent of abnormalities that we observed in root cells overexpressing AP2C3, including defects in spindle pole alignment and chromosomal separation. EB1c might be directly regulated through MAPK phosphorylation, and inhibition of this phosphorylation through AP2C3 overexpression has the consequence of defective attachment of kinetochore microtubules to chromosomes. There is a growing body of evidence indicating that functions of EB1 proteins are regulated by phosphorylation in animal cells (Tamura & Draviam, 2012). Moreover, EB1 protein is important for correct attachment of spindle microtubules to kinetochores, and depletion of EB1 in animal cells results in defective spindle positioning, metaphase chromosomal congression and separation in metazoan cells (Draviam *et al.*, 2006).

MAP kinase signalling at cytokinesis involves the well-characterised NACK-PQR MAPK pathway that targets MAP65 proteins for phosphorylation (Calderini *et al.*, 1998; Sasabe *et al.*, 2011). Phosphorylation of MAP65-1 by MAP kinases regulates its microtubule bundling function and ensures phragmoplast microtubule dynamics required for phragmoplast expansion and cytokinesis progression (Sasabe *et al.*, 2006). We identified through inducible silencing a role for γ-tubulin in late mitotic events (Binarova *et al.*, 2006). It is suggested that there are other microtubule-associated substrates of the cytokinetic MAPK pathway (Sasabe & Machida, 2012); however, whether this pathway also targets γ-tubulin complexes or EB1c for regulation is not known. While the single *mpk6-2* mutant develops normally under our control conditions, simultaneous inactivation of MPK3, MPK4 and MPK6 through the overexpression of AP2C3 MAPK phosphatase led to strong cell division defects including spindle positioning, chromosomal congression, separation and misalignment of the cell

division sites. This indicates synergistic and partially overlapping mitotic functions for MPK3, MPK4 and MPK6. These data were supported by our observation of similar types of aberrant mitotic figures in cells where MAP kinase activity was reduced by specific MEK inhibitor U0126 treatment.

MPK6 was suggested to associate with membrane vesicles (Muller *et al.*, 2010) and the pathway downstream of YODA was shown to affect cortical microtubule organisation and auxin biosynthesis (Smekalova *et al.*, 2014). YODA is part of a meristematic developmental pathway downstream of the ERECTA receptor-like kinase, which activates MKK4/MKK5 and then MPK3/MPK6 to regulate cell proliferation and plant architecture (Meng *et al.*, 2012). MPK6 has an inhibitory effect on cell proliferation, as indicated by enlarged seeds and faster growing roots of the *mpk6* mutant (Lopez-Bucio *et al.*, 2014). Thus MPK6 might impact not only on microtubular organisation, but also on cell cycle progression. In agreement, it was shown that inactivation of MAPKs through the over-expression of AP2C3 led to over-proliferation of stomatal lineage cells and to increased CDK activity (Umbrasaite *et al.*, 2010).

MPK6 is a part of multiple MAPK signalling pathways in plants that are involved in both developmental and stress signalling. Of special interest is the activation of MPK6 by ROS (Wang *et al.*, 2013). ROS activated MPK6 phosphorylates nitrate reductase NIA2, leading to an increase in NO production (Wang *et al.*, 2010). Nitrosative stress induces depolymerization of microtubules in mammalian cells (Laguinge *et al.*, 2004); mild nitrosative stress due to treatment with NO_2-Tyr, a source of exogenous N-tyrosine, affects microtubule organisation in *Arabidopsis* plants (Lipka & Muller, 2014). Nitration of tyrosine on α-tubulin may change the tyrosination/detyrosination cycle of microtubules with an impact on kinesin or MAPs interactions with microtubules (Blume *et al.*, 2013). Previously, it was reported that the *mpk6* mutant is more sensitive to NO donors concerning root development (Wang *et al.*, 2010) and now we show that there is an altered sensitivity to maintaining the cell division plane upon NO_2-Tyr treatment in this mutant, compared to wild type. This suggests that tyrosine nitration regulating microtubule organization and the MPK6 pathway act on a common mechanism to regulate cell division. Activation of the MPK6 pathway upon stress might play an important role in limiting the disruption of microtubular organisation. NIA2, a target of MPK6 signalling under ROS stress (Wang *et al.*, 2010), was shown to interact with 14-3-3ω in proteomic studies and in a yeast two hybrid assay (Kanamaru *et al.*, 1999; Chang *et al.*, 2009). Our LC-MALDI-TOF MS/MS analysis of MPK6 complexes also

identified 14-3-3ω protein as an interactor in proliferating *Arabidopsis* cells (Table S1). We validated this interaction by Western blot (Fig. S5). Because 14-3-3 proteins function as adaptors between phosphorylated proteins and specific cellular compartments or protein complexes (Gokirmak *et al.*, 2010), 14-3-3ω might provide a central adapter mechanism for MPK6 both towards substrates and for localisation on microtubules. It is possible that active MPK6 is brought to the γ-tubulin complexes or other microtubular substrates through interactions with 14-3-3ω.

MPK6 is a multifunctional MAPK utilised both in developmental and stress responses. It is not clear whether this versatility is due to its participation in many different pathways and complexes or if the same module is used in different contexts. Identification of novel interactors and phosphorylated substrates will be essential to address these questions. Our data show that γ-tubulin complexes and EB1c protein are two novel partners for MPK6 signalling and we show that MPK6 plays important roles in regulating the mitotic cytoskeleton and plane of cell division, particularly under stress.

Acknowledgements

The work was supported by Grant from Grant Agency of the Czech Republic P501-12-2333 to PB, Grant MSMT Kontakt 7AMB13AT013 to PB and IM, CH-3-ŠMM-01/10 to IM, Grant OTKA NN111085 to TM. Authors contribution: LK biochemistry, microscopy, phenotype analysis, manuscript preparation, HK cloning, biochemistry, microscopy, SKN cloning, in vitro translation and phosphorylation, JV biochemistry, PH proteomics, TM in vitro translation, IM cloning, transformation, LB designing of experiments, data interpretation and manuscript preparation, PB designing of experiments, data interpretation and manuscript preparation. We thank to Prof. R. J. Ferl (Univ. of Florida) for 4B9 antibody. We also thank to Gabriela Kočárová for technical assistance.

References

Beck M, Komis G, Ziemann A, Menzel D, Samaj J. 2011. Mitogen-activated protein kinase 4 is involved in the regulation of mitotic and cytokinetic microtubule transitions in Arabidopsis thaliana. *The New phytologist* **189**(4): 1069-1083.

626 **Binarova P, Cenklova V, Hause B, Kubatova E, Lysak M, Dolezel J, Bogre L, Draber P.**
627 **2000.** Nuclear gamma-tubulin during acentriolar plant mitosis. *Plant Cell* **12**(3): 433-442.
628 **Binarova P, Cenklova V, Prochazkova J, Doskocilova A, Volc J, Vrlik M, Bogre L. 2006.**
629 Gamma-tubulin is essential for acentrosomal microtubule nucleation and coordination of late
630 mitotic events in Arabidopsis. *Plant Cell* **18**(5): 1199-1212.
631 **Blume YB, Krasylenko YA, Demchuk OM, Yemets AI. 2013.** Tubulin tyrosine nitration
632 regulates microtubule organization in plant cells. *Frontiers in plant science* **4**: 530.
633 **Bouissou A, Verollet C, de Forges H, Haren L, Bellaiche Y, Perez F, Merdes A,**
634 **Raynaud-Messina B. 2014.** gamma-Tubulin Ring Complexes and EB1 play antagonistic
635 roles in microtubule dynamics and spindle positioning. *The EMBO journal* **33**(2): 114-128.
636 **Calderini O, Bogre L, Vicente O, Binarova P, Heberle-Bors E, Wilson C. 1998.** A cell
637 cycle regulated MAP kinase with a possible role in cytokinesis in tobacco cells. *J Cell Sci*
638 **111**(Pt 20): 3091-3100.
639 **Colello D, Mathew S, Ward R, Pumiglia K, LaFlamme SE. 2012.** Integrins regulate
640 microtubule nucleating activity of centrosome through mitogen-activated protein
641 kinase/extracellular signal-regulated kinase kinase/extracellular signal-regulated kinase
642 (MEK/ERK) signaling. *The Journal of biological chemistry* **287**(4): 2520-2530.
643 **Cuschieri L, Miller R, Vogel J. 2006.** Gamma-tubulin is required for proper recruitment and
644 assembly of Kar9-Bim1 complexes in budding yeast. *Mol Biol Cell* **17**(10): 4420-4434.
645 **Draviam VM, Shapiro I, Aldridge B, Sorger PK. 2006.** Misorientation and reduced
646 stretching of aligned sister kinetochores promote chromosome missegregation in EB1- or
647 APC-depleted cells. *The EMBO journal* **25**(12): 2814-2827.
648 **Drykova D, Cenklova V, Sulimenko V, Volc J, Draber P, Binarova P. 2003.** Plant
649 gamma-tubulin interacts with alphabeta-tubulin dimers and forms membrane-associated
650 complexes. *Plant Cell* **15**(2): 465-480.
651 **Ellis BE. 2012.** Postal code for a plant MAPK. *The Biochemical journal* **446**(2): e5-7.
652 **Gokirmak T, Paul AL, Ferl RJ. 2010.** Plant phosphopeptide-binding proteins as signaling
653 mediators. *Current opinion in plant biology* **13**(5): 527-532.
654 **Hagan IM. 2008.** The spindle pole body plays a key role in controlling mitotic commitment
655 in the fission yeast Schizosaccharomyces pombe. *Biochemical Society transactions* **36**(Pt 5):
656 1097-1101.

Hord CL, Sun YJ, Pillitteri LJ, Torii KU, Wang H, Zhang S, Ma H. 2008. Regulation of Arabidopsis early anther development by the mitogen-activated protein kinases, MPK3 and MPK6, and the ERECTA and related receptor-like kinases. *Molecular plant* **1**(4): 645-658.

Horejsi B, Vinopal S, Sladkova V, Draberova E, Sulimenko V, Sulimenko T, Vosecka V, Philimonenko A, Hozak P, Katsetos CD, et al. 2012. Nuclear gamma-tubulin associates with nucleoli and interacts with tumor suppressor protein C53. *J Cell Physiol* **227**(1): 367-382.

Chang IF, Curran A, Woolsey R, Quilici D, Cushman JC, Mittler R, Harmon A, Harper JF. 2009. Proteomic profiling of tandem affinity purified 14-3-3 protein complexes in Arabidopsis thaliana. *Proteomics* **9**(11): 2967-2985.

Kanamaru K, Wang R, Su W, Crawford NM. 1999. Ser-534 in the hinge 1 region of Arabidopsis nitrate reductase is conditionally required for binding of 14-3-3 proteins and in vitro inhibition. *The Journal of biological chemistry* **274**(7): 4160-4165.

Karimi M, Inze D, Depicker A. 2002. GATEWAY vectors for Agrobacterium-mediated plant transformation. *Trends in plant science* **7**(5): 193-195.

Komaki S, Abe T, Coutuer S, Inze D, Russinova E, Hashimoto T. 2010. Nuclear-localized subtype of end-binding 1 protein regulates spindle organization in Arabidopsis. *J Cell Sci* **123**(Pt 3): 451-459.

Komis G, Illes P, Beck M, Samaj J. 2011. Microtubules and mitogen-activated protein kinase signalling. *Current opinion in plant biology* **14**(6): 650-657.

Kosetsu K, Matsunaga S, Nakagami H, Colcombet J, Sasabe M, Soyano T, Takahashi Y, Hirt H, Machida Y. 2010. The MAP kinase MPK4 is required for cytokinesis in Arabidopsis thaliana. *The Plant cell* **22**(11): 3778-3790.

Laguinge LM, Lin S, Samara RN, Salesiotis AN, Jessup JM. 2004. Nitrosative stress in rotated three-dimensional colorectal carcinoma cell cultures induces microtubule depolymerization and apoptosis. *Cancer research* **64**(8): 2643-2648.

Larkin MA, Blackshields G, Brown NP, Chenna R, McGettigan PA, McWilliam H, Valentin F, Wallace IM, Wilm A, Lopez R, et al. 2007. Clustal W and Clustal X version 2.0. *Bioinformatics* **23**(21): 2947-2948.

Lee SE, Kim JH, Kim NH. 2007. Inactivation of MAPK affects centrosome assembly, but not actin filament assembly, in mouse oocytes maturing in vitro. *Mol Reprod Dev* **74**(7): 904-911.

689 **Lipka E, Muller S. 2014.** Nitrosative stress triggers microtubule reorganization in
690 Arabidopsis thaliana. *Journal of experimental botany* **65**(15): 4177-4189.
691 **Liu Y, Zhang S. 2004.** Phosphorylation of 1-aminocyclopropane-1-carboxylic acid synthase
692 by MPK6, a stress-responsive mitogen-activated protein kinase, induces ethylene biosynthesis
693 in Arabidopsis. *The Plant cell* **16**(12): 3386-3399.
694 **Lopez-Bucio JS, Dubrovsky JG, Raya-Gonzalez J, Ugartechea-Chirino Y, Lopez-Bucio**
695 **J, de Luna-Valdez LA, Ramos-Vega M, Leon P, Guevara-Garcia AA. 2014.** Arabidopsis
696 thaliana mitogen-activated protein kinase 6 is involved in seed formation and modulation of
697 primary and lateral root development. *Journal of experimental botany* **65**(1): 169-183.
698 **Meister M, Tomasovic A, Banning A, Tikkanen R. 2013.** Mitogen-Activated Protein
699 (MAP) Kinase Scaffolding Proteins: A Recount. *International journal of molecular sciences*
700 **14**(3): 4854-4884.
701 **Meng X, Wang H, He Y, Liu Y, Walker JC, Torii KU, Zhang S. 2012.** A MAPK cascade
702 downstream of ERECTA receptor-like protein kinase regulates Arabidopsis inflorescence
703 architecture by promoting localized cell proliferation. *The Plant cell* **24**(12): 4948-4960.
704 **Mishra RK, Chakraborty P, Arnaoutov A, Fontoura BM, Dasso M. 2010.** The Nup107-
705 160 complex and gamma-TuRC regulate microtubule polymerization at kinetochores. *Nat*
706 *Cell Biol* **12**(2): 164-169.
707 **Muller J, Beck M, Mettbach U, Komis G, Hause G, Menzel D, Samaj J. 2010.**
708 Arabidopsis MPK6 is involved in cell division plane control during early root development,
709 and localizes to the pre-prophase band, phragmoplast, trans-Golgi network and plasma
710 membrane. *The Plant journal : for cell and molecular biology* **61**(2): 234-248.
711 **Nagy SK, Meszaros T. 2014.** In vitro translation-based protein kinase substrate
712 identification. *Methods in molecular biology* **1118**: 231-243.
713 **Nishihama R, Ishikawa M, Araki S, Soyano T, Asada T, Machida Y. 2001.** The NPK1
714 mitogen-activated protein kinase kinase kinase is a regulator of cell-plate formation in plant
715 cytokinesis. *Genes Dev* **15**(3): 352-363.
716 **Olmsted ZT, Colliver AG, Riehlman TD, Paluh JL. 2014.** Kinesin-14 and kinesin-5
717 antagonistically regulate microtubule nucleation by gamma-TuRC in yeast and human cells.
718 *Nature communications* **5**: 5339.
719 **Ou XH, Li S, Xu BZ, Wang ZB, Quan S, Li M, Zhang QH, Ouyang YC, Schatten H,**
720 **Xing FQ, et al. 2010.** p38alpha MAPK is a MTOC-associated protein regulating spindle

721 assembly, spindle length and accurate chromosome segregation during mouse oocyte meiotic
722 maturation. *Cell Cycle* **9**(20): 4130-4143.
723 **Popescu SC, Popescu GV, Bachan S, Zhang Z, Gerstein M, Snyder M, Dinesh-Kumar**
724 **SP. 2009.** MAPK target networks in Arabidopsis thaliana revealed using functional protein
725 microarrays. *Genes & Development* **23**(1): 80-92.
726 **Pozo-Guisado E, Casas-Rua V, Tomas-Martin P, Lopez-Guerrero AM, Alvarez-**
727 **Barrientos A, Martin-Romero FJ. 2013.** Phosphorylation of STIM1 at ERK1/2 target sites
728 regulates interaction with the microtubule plus-end binding protein EB1. *Journal of cell*
729 *science* **126**(Pt 14): 3170-3180.
730 **Sasabe M, Kosetsu K, Hidaka M, Murase A, Machida Y. 2011.** Arabidopsis thaliana
731 MAP65-1 and MAP65-2 function redundantly with MAP65-3/PLEIADE in cytokinesis
732 downstream of MPK4. *Plant signaling & behavior* **6**(5): 743-747.
733 **Sasabe M, Machida Y. 2012.** Regulation of organization and function of microtubules by the
734 mitogen-activated protein kinase cascade during plant cytokinesis. *Cytoskeleton* **69**(11): 913-
735 918.
736 **Sasabe M, Soyano T, Takahashi Y, Sonobe S, Igarashi H, Itoh TJ, Hidaka M, Machida**
737 **Y. 2006.** Phosphorylation of NtMAP65-1 by a MAP kinase down-regulates its activity of
738 microtubule bundling and stimulates progression of cytokinesis of tobacco cells. *Genes &*
739 *Development* **20**(8): 1004-1014.
740 **Sauer M, Paciorek T, Benkova E, Friml J. 2006.** Immunocytochemical techniques for
741 whole-mount in situ protein localization in plants. *Nature protocols* **1**(1): 98-103.
742 **Sethi V, Raghuram B, Sinha AK, Chattopadhyay S. 2014.** A Mitogen-Activated Protein
743 Kinase Cascade Module, MKK3-MPK6 and MYC2, Is Involved in Blue Light-Mediated
744 Seedling Development in Arabidopsis. *The Plant cell* **26**(8): 3343-3357.
745 **Smekalova V, Luptovciak I, Komis G, Samajova O, Ovecka M, Doskocilova A, Takac T,**
746 **Vadovic P, Novak O, Pechan T, et al. 2014.** Involvement of YODA and mitogen activated
747 protein kinase 6 in Arabidopsis post-embryogenic root development through auxin up-
748 regulation and cell division plane orientation. *The New phytologist* **203**(4): 1175-1193.
749 **Smertenko AP, Chang HY, Sonobe S, Fenyk SI, Weingartner M, Bogre L, Hussey PJ.**
750 **2006.** Control of the AtMAP65-1 interaction with microtubules through the cell cycle.
751 *Journal of cell science* **119**(Pt 15): 3227-3237.
752 **Sorensson C, Lenman M, Veide-Vilg J, Schopper S, Ljungdahl T, Grotli M, Tamas MJ,**
753 **Peck SC, Andreasson E. 2012.** Determination of primary sequence specificity of

Arabidopsis MAPKs MPK3 and MPK6 leads to identification of new substrates. *The Biochemical journal* **446**(2): 271-278.

Sun QY, Lai L, Wu GM, Park KW, Day BN, Prather RS, Schatten H. 2001. Microtubule assembly after treatment of pig oocytes with taxol: correlation with chromosomes, gamma-tubulin, and MAP kinase. *Mol Reprod Dev* **60**(4): 481-490.

Tamura N, Draviam VM. 2012. Microtubule plus-ends within a mitotic cell are 'moving platforms' with anchoring, signalling and force-coupling roles. *Open biology* **2**(11): 120132.

Tomastikova E, Cenklova V, Kohoutova L, Petrovska B, Vachova L, Halada P, Kocarova G, Binarova P. 2012. Interactions of an Arabidopsis RanBPM homologue with LisH-CTLH domain proteins revealed high conservation of CTLH complexes in eukaryotes. *BMC plant biology* **12**: 83.

Toufighi K, Brady SM, Austin R, Ly E, Provart NJ. 2005. The Botany Array Resource: e-Northerns, Expression Angling, and promoter analyses. *Plant J* **43**(1): 153-163.

Umbrasaite J, Schweighofer A, Kazanaviciute V, Magyar Z, Ayatollahi Z, Unterwurzacher V, Choopayak C, Boniecka J, Murray JA, Bogre L, et al. 2010. MAPK phosphatase AP2C3 induces ectopic proliferation of epidermal cells leading to stomata development in Arabidopsis. *PLoS ONE* **5**(12): e15357.

Van Damme D, Bouget FY, Van Poucke K, Inze D, Geelen D. 2004. Molecular dissection of plant cytokinesis and phragmoplast structure: a survey of GFP-tagged proteins. *Plant J* **40**(3): 386-398.

van den Berg S, Lofdahl PA, Hard T, Berglund H. 2006. Improved solubility of TEV protease by directed evolution. *Journal of biotechnology* **121**(3): 291-298.

Wang H, Liu Y, Bruffett K, Lee J, Hause G, Walker JC, Zhang S. 2008. Haplo-insufficiency of MPK3 in MPK6 mutant background uncovers a novel function of these two MAPKs in Arabidopsis ovule development. *The Plant cell* **20**(3): 602-613.

Wang H, Ngwenyama N, Liu Y, Walker JC, Zhang S. 2007. Stomatal development and patterning are regulated by environmentally responsive mitogen-activated protein kinases in Arabidopsis. *The Plant cell* **19**(1): 63-73.

Wang P, Du Y, Li Y, Ren D, Song CP. 2010. Hydrogen peroxide-mediated activation of MAP kinase 6 modulates nitric oxide biosynthesis and signal transduction in Arabidopsis. *The Plant cell* **22**(9): 2981-2998.

Wang P, Du Y, Zhao X, Miao Y, Song CP. 2013. The MPK6-ERF6-ROS-responsive cis-acting Element7/GCC box complex modulates oxidative gene transcription and the oxidative response in Arabidopsis. *Plant physiology* **161**(3): 1392-1408.

Xu J, Zhang S. 2014. Mitogen-activated protein kinase cascades in signaling plant growth and development. *Trends in plant science*.

Figure legends

Fig. 1 MPK6 is present with microtubules and associates with γ-tubulin

(a) γ-Tubulin co-purified with MPK6. MPK6 IP – eluate after immunoprecipitation with anti-MPK6 antibody, PS IP – control eluate using pre-immune serum, IN – extract S20; (b) MPK6 co-purified with γ-tubulin. γ-Tub IP – immunoprecipitate using anti-γ-tubulin antibody; PS IP – control immunoprecipitate using pre-immune serum, IN – extract S20; (a, b) Western blots probed with anti-γ-tubulin and anti-MPK6 antibody. (c) MPK6 and p-ERK were pulled down with *in vitro* taxol-polymerized plant microtubules. Plant microtubules were polymerized from high speed supernatant S70 (IN) by taxol-driven polymerization and analysed by antibodies against α-tubulin, MAP65-1, EB1, γ-tubulin, GCP4 protein, MPK6, and p-ERK. S/MT + Tax: supernatant/microtubular pellet after taxol treatment and without supplementing the assay with taxol (S/MT –Tax). (d) MPK6 co-purified with γ-tubulin when proteins pulled down with plant microtubules were used as an input (IN = MT + Tax). γ-Tub IP – immunoprecipitate using anti-γ-tubulin antibody, PS IP – control immunoprecipitate using pre-immune serum. Western blots probed with anti-MPK6 and anti-γ-tubulin antibody.

Fig. 2 Localisation of MPK6 and γ-tubulin with mitotic microtubules

(a-g) Whole mount immunofluorescence labelling of dividing cells of *Arabidopsis* root. (a) MPK6 signal on pre-prophase band (arrows), with metaphase spindles (arrowheads), and with phragmoplast area (asterisk). (b) Signal for p-ERK with metaphase spindles (arrowheads) and with phragmoplast area (asterisk), but hardly with pre-prophase bands (arrows). (c) While MPK6 besides its kinetochore fibres localisation (arrowheads) was also in midzone (arrow), (d) signal for p-ERK in anaphase was mainly on shortening kinetochore fibres (arrowheads). (e) Signal for p-ERK localised on shortening kinetochore fibres with γ-tubulin in anaphase. (f) In telophase, both p-ERK signal and γ-tubulin were present on the remnants of kinetochore

817 microtubules and with early phragmoplast. (g) Later in cytokinesis, p-ERK signal was in the
818 phragmoplast area. Bars (a-g), 5 μm.
819
820 **Fig. 3 Signal for p-ERK follows dynamic localisation of γ-tubulin in anaphase/telophase**
821 **transition**
822 (a) In anaphase, p-ERK signal localised with γ-tubulin on shortening kinetochore fibres
823 (arrowheads), while γ-tubulin was also partially on newly forming phragmoplast microtubules
824 (arrows). (b) In later anaphase, p-ERK signal translocate to γ-tubulin positive area on newly
825 forming phragmoplast (arrows) but compared to γ-tubulin the signal for p-ERK was less
826 intense (intensity profile). (c) In telophase, both p-ERK signal and γ-tubulin were present on
827 the remnants of kinetochore microtubules (arrowheads) and stained early phragmoplast but
828 p-ERK signal delayed behind γ-tubulin signal in newly formed phragmoplast as shown by
829 intensity profile. (d) Later in telophase, both p-ERK signal and γ-tubulin on the remnants of
830 kinetochore microtubules gradually diminished and both proteins were located with early
831 phragmoplast (arrows) as shown by intensity profile. (e) In anaphase, MPK6 signal strong in
832 midzone (arrow), weaker signal with shortening kinetochore fibres (arrowheads). (f) In
833 telophase, MPK6 signal was present mainly in midzone in phragmoplast area. Double
834 immunofluorescence labelling of *Arabidopsis* cells: p-ERK (red), MPK6 (red), γ-tubulin
835 (green), DNA stained by DAPI (blue). Intensity profiles: x axis shows length in μm (number 1
836 indicates start of the line used for measurement corresponding to point 0); y axis shows
837 relative intensity; red line for p-ERK or MPK6, respectively, green line for γ-tubulin. Bars (a-
838 f), 5 μm.
839
840 **Fig. 4 MPK6 phosphorylates and interacts with microtubule plus end protein EB1c**
841 (a) Phosphorylation of EB1c *in vitro* by MKK4-activated MPK6. EB1c, was phosphorylated
842 by active MPK6 *in vitro*, while EB1a, γ-tubulin, and GCP4 were not phosphorylated.
843 Autoradiograph and Coomassie-stained gel are shown. (b) MPK6 co-purified with
844 endogenous EB1s. EB1 IP – immunoprecipitate using anti-EB1 antibody, PS IP – control
845 immunoprecipitate using pre-immune serum, IN – extract S20; Western blot probed with anti-
846 MPK6 antibody. (c) MPK6 co-purified with EB1c-GFP. IN – extract from EB1c-GFP cell
847 culture, EB1c-GFP IP – immunoprecipitate using GFP trap from EB1c-GFP cell culture, ctrl
848 IP – control immunoprecipitate from Ler culture; Western blots probed with anti-MPK6 and
849 anti-EB1 antibody. (d) EB1c-GFP and endogenous EB1c co-purified with MPK6. MPK6 IP –

eluate after immunoprecipitation with anti-MPK6 antibody from EB1c-GFP cell culture; PS IP – control eluate using pre-immune serum, IN – extract S20; Western blots probed with anti-EB1 and anti-GFP antibody. (e) Reduction of p-ERK signal after U0126 treatment in extract S20 from Arabidopsis cell culture. Western blot probed with p-ERK antibody. (f) EB1c-GFP immunopurified from EB1c-GFP cell culture extract is phosphorylated and its phosphorylation is reduced after U0126 treatment. Purified EB1c-GFP without (-) and with (+) lambda protein phosphatase (lambda PP) treatment; EB1c-GFP purified from cell culture without U0126 (-) and with U0126 treatment (+). Western blots probed with anti-p-Thr antibody.

Fig. 5 Localisation of p-ERK and MPK6 with microtubule plus end protein EB1c

(a) In metaphase, EB1c-GFP signal was with spindle and prominent near to kinetochores (arrows) where it partially localised with p-ERK signal (see intensity profile). (b) In late anaphase, p-ERK and EB1c-GFP localised together on shortening kinetochore fibres (arrowheads); while EB1c-GFP signal was accumulated in midline of newly forming phragmoplast (arrow), p-ERK was near to chromatin on newly formed phragmoplast. (c) In telophase, both p-ERK signal and EB1c-GFP were present on the remnants of kinetochore microtubules (arrowheads); EB1c-GFP was localised in phragmoplast midline (arrow) and p-ERK with phragmoplast microtubules facing to separated chromatin. (d) In metaphase, MPK6 and EB1c-GFP were within spindle and near to kinetochores. (e, f) In late anaphase and telophase, MPK6 signal was in midzone and with shortening kinetochore fibres (arrowheads). Double immunofluorescence labelling of *Arabidopsis* cells: EB1c-GFP (green), p-ERK (red), MPK6 (red), DNA stained by DAPI (blue). Intensity profiles: x axis shows length in μm (number 1 indicates start of the line used for measurement corresponding to point 0); y axis shows relative intensity; red line for p-ERK or MPK6, respectively, green line for EB1c-GFP. Bars (a-f), 5 μm.

Fig. 6 A root development is more affected after NO_2-Tyr treatment in *mpk6-2* mutants compared to WT plants

(a) Representative images of 11-d-old WT Col-0 and *mpk6-2* mutants grown on control medium or on 0.5 μM NO_2-Tyr supplemented medium. NO_2-Tyr treatment affected root development: primary roots growth was retarded in WT Col-0 and stronger effect was observed in *mpk6-2* mutants. (b-e) Whole mount immunofluorescence labelling: α-tubulin

(green), DAPI (blue) of 11-d-old control WT and *mpk6-2* seedlings and NO_2-Tyr treated WT and *mpk6-2* seedlings. (b) Regular files with mitotic spindle and phragmoplast in WT Col-0 control. (c) Obliqued mitotic spindle in WT Col-0 grown on NO_2-Tyr. Compare to *mpk6-2* grown under control conditions (d), disturbed cell files, misaligned spindles (arrow) and phragmoplast (arrowhead) were observed in *mpk6-2* seedlings grown under NO_2-Tyr (e). Bars (b-e), 5 μm.

Fig. 7 Mitotic and cytokinetic defects in dividing cells of roots of AP2C3 oe plants

(a-e) Whole mount immunofluorescence labelling of 7-d-old AP2C3 plants. (a) Typical examples of the WT and AP2C3 oe primary roots. Clusters of dividing cells with misaligned cell plates (arrowheads), irregular cell files, and multinuclear cell (arrow) observed in AP2C3 roots. (b) Impaired chromosome congression in metaphase (arrowhead). (c) Anaphase with lagging chromosome (arrowhead), aberrant anaphase/telophase with two clusters of condensed chromosomes surrounded by microtubules (arrow), lobed nucleus (asterisk). (d) Misaligned anaphase spindle (arrow) and phragmoplast (e, arrow). α-tubulin (green), KNOLLE (red), DAPI (blue). (f) Percentage of aberrant mitosis and phragmoplasts in AP2C3 oe roots: AP2C3 oe (blue bars), WT (red bars), n under bars represents number of analysed figures, error bars indicate SD, ** indicates significant difference between WT and AP2C3 for the category at $p < 0.01$. Bars (a), 20 μm; (b-e), 5 μm.

Fig. 8 Treatment of Arabidopsis cells with MEK inhibitor U0126 reduced levels of p-ERK labelled active MAP kinases with polymerized microtubules and induced mitotic defects

(a) Signal for p-ERK was reduced on microtubules polymerized *in vitro* from U0126 treated cells. Western blots were probed with antibodies against α-tubulin, p-ERK, MAP65-1, MPK6, EB1, and γ-tubulin. (b-f) Immunofluorescence labelling showing aberrant chromosome congression and separation in U0126 treated *Arabidopsis* cells (b) Long spindle with thick kinetochore fibres (arrows) and γ-tubulin accumulated on the poles. (c) Another z-stack of the spindle from (b) showing failure of chromosome congression and unattached chromosomes (arrowheads). (d) Cells with highly bundled phragmoplast microtubules (arrow) and with only weak signal for γ-tubulin and nuclei with already decondensed chromatin (arrowheads). (e) Aberant anaphase spindle with long bundled astral microtubules (arrow) and lagging chromosomes (arrowheads). (f) Telophase with escaped lagged chromosomes (arrows). α-

916 tubulin (green), γ-tubulin (red) or phospho-Histone H3 (red), DNA stained by DAPI (blue).
917 Bars (b-f), 5 μm.
918
919 **Supporting Information**
920 **Fig. S1** Antibody p-ERK recognises predominantly MPK6 on Western blots and in
921 *Arabidopsis* cells
922 **Fig. S2** MPK6 and p-ERK labelling in Taxol and APM treated cells
923 **Fig. S3** Multiple sequence alignment of *Arabidopsis* EB1 proteins
924 **Fig. S4** Mitotic activity and alignment of spindle and phragmoplast is more affected after
925 NO_2-Tyr treatment in 10-d-old *mpk6-2* mutants compared to WT Col-0
926 **Fig. S5** 14-3-3ω co-purified with MPK6
927 **Table S1** Proteins co-purified with MPK6 from *Arabidopsis* proliferating cultured cells
928 identification by LC-MALDI-TOF mass spectrometry
929 **Methods S1** Protein digestion and LC MALDI-TOF mass spectrometry

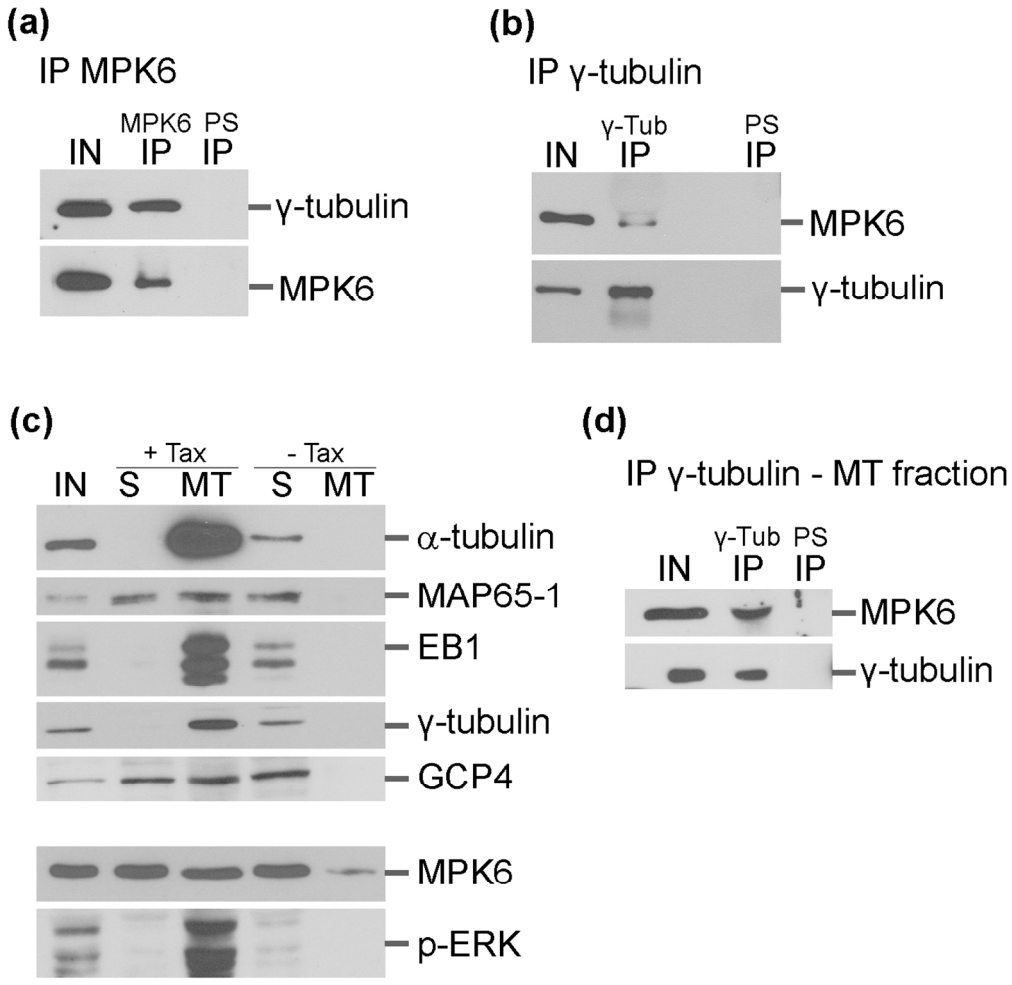

Fig1
120x117mm (300 x 300 DPI)

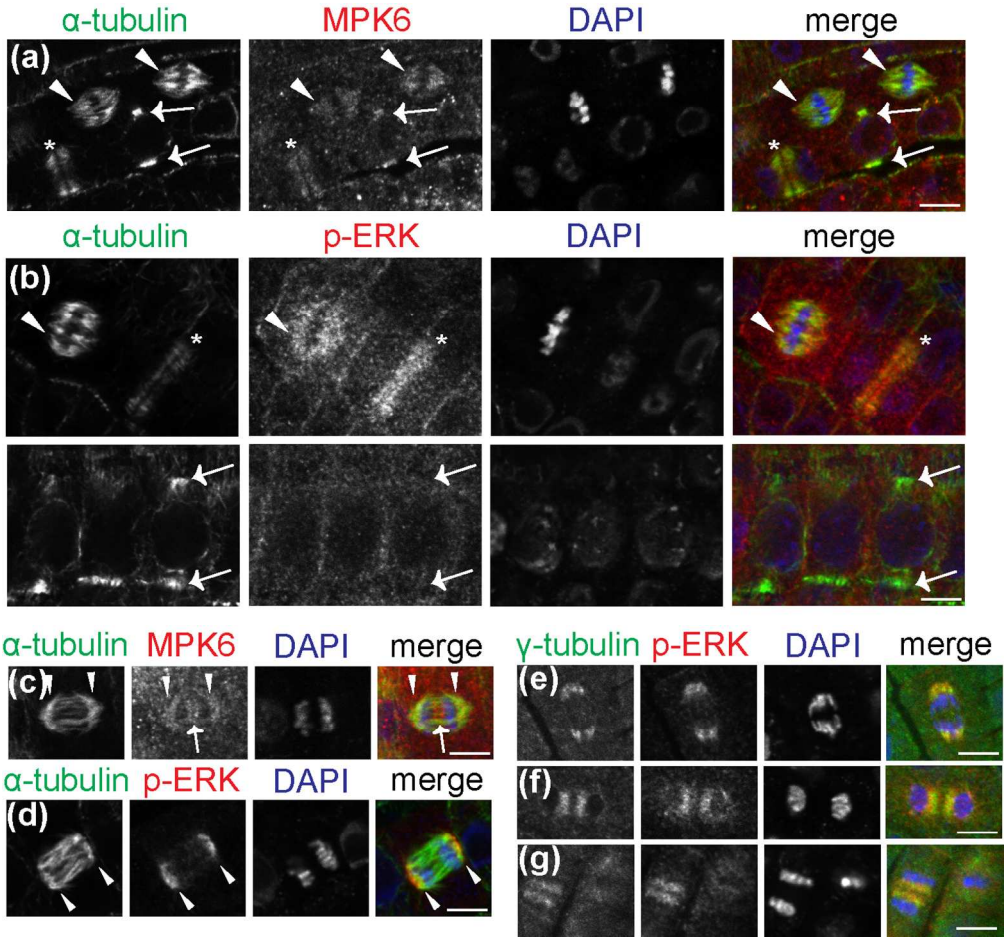

Fig2
129x120mm (300 x 300 DPI)

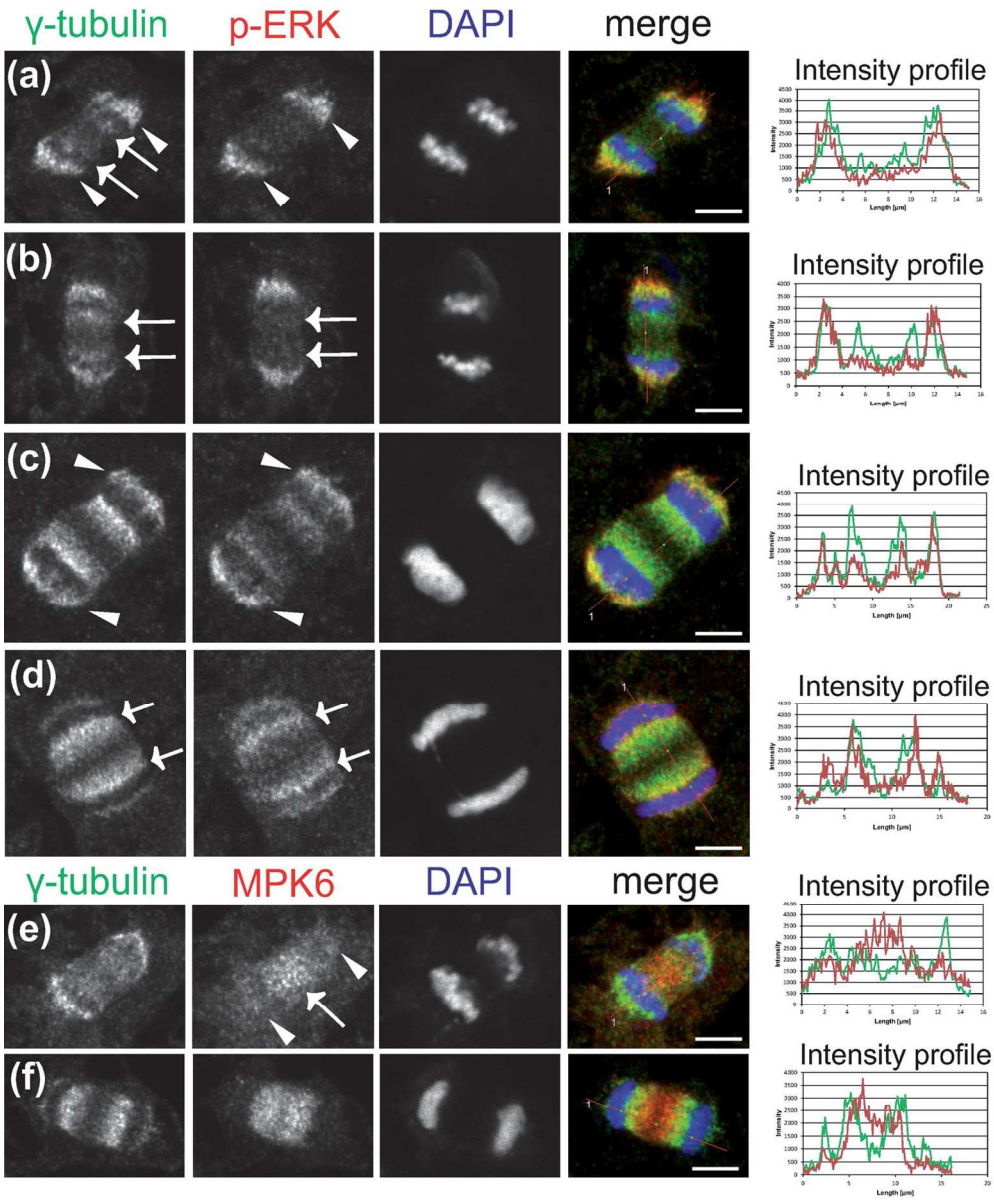

Fig3
133x160mm (300 x 300 DPI)

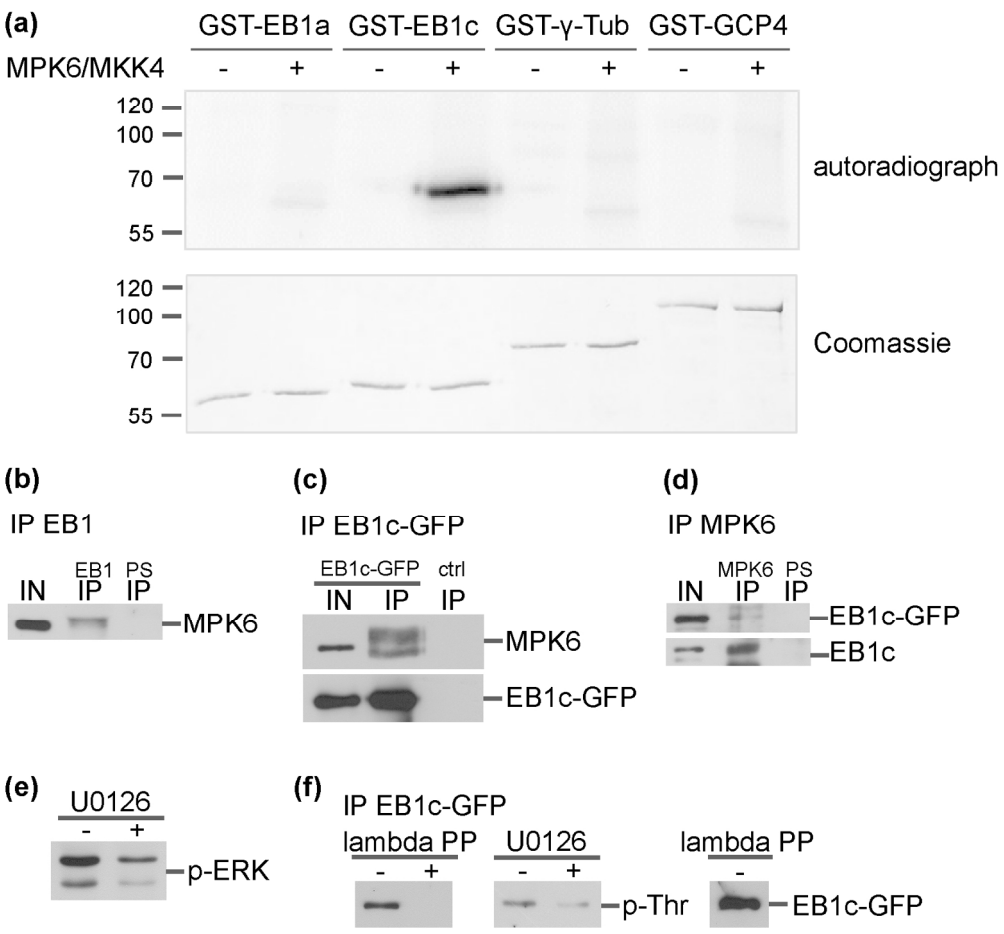

Fig4
153x141mm (300 x 300 DPI)

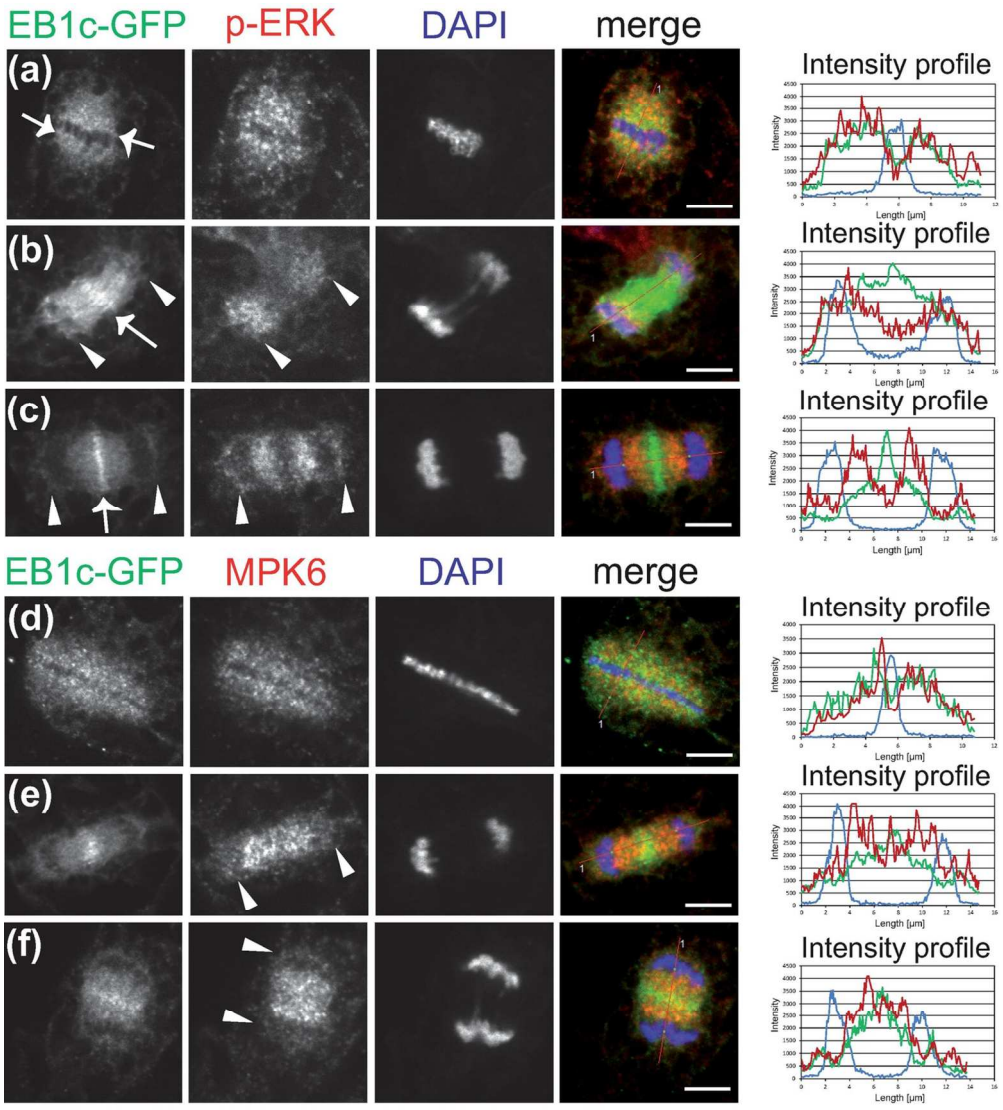

Fig5
124x138mm (300 x 300 DPI)

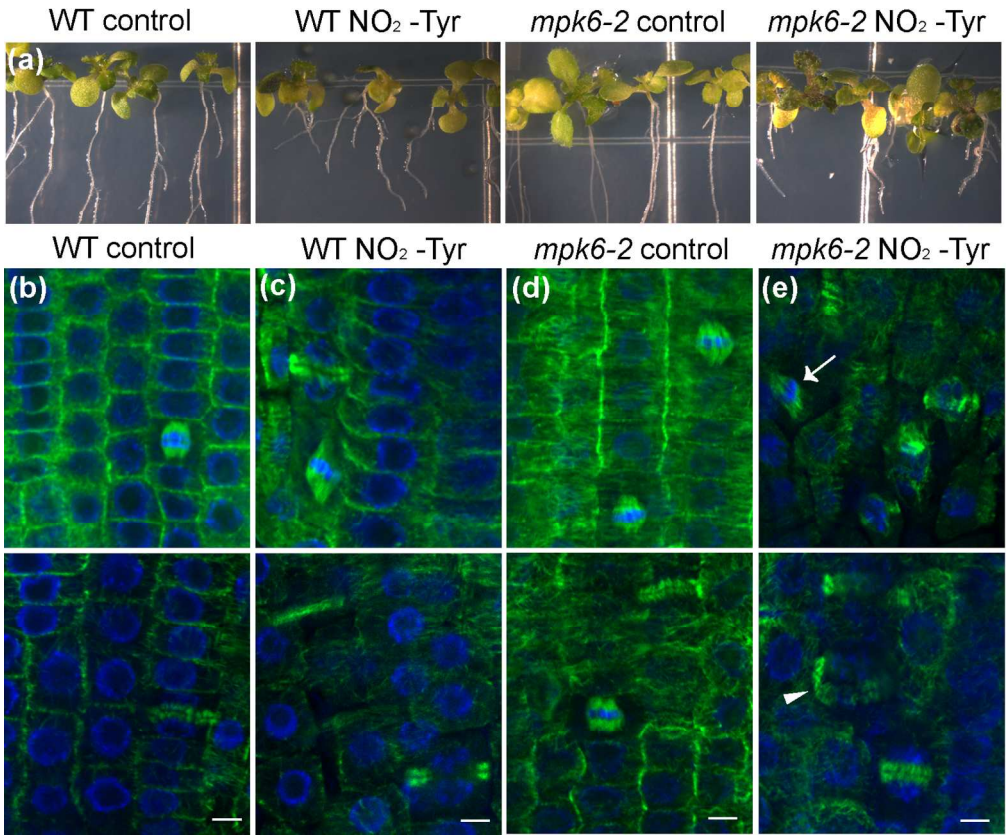

Fig6
142x118mm (300 x 300 DPI)

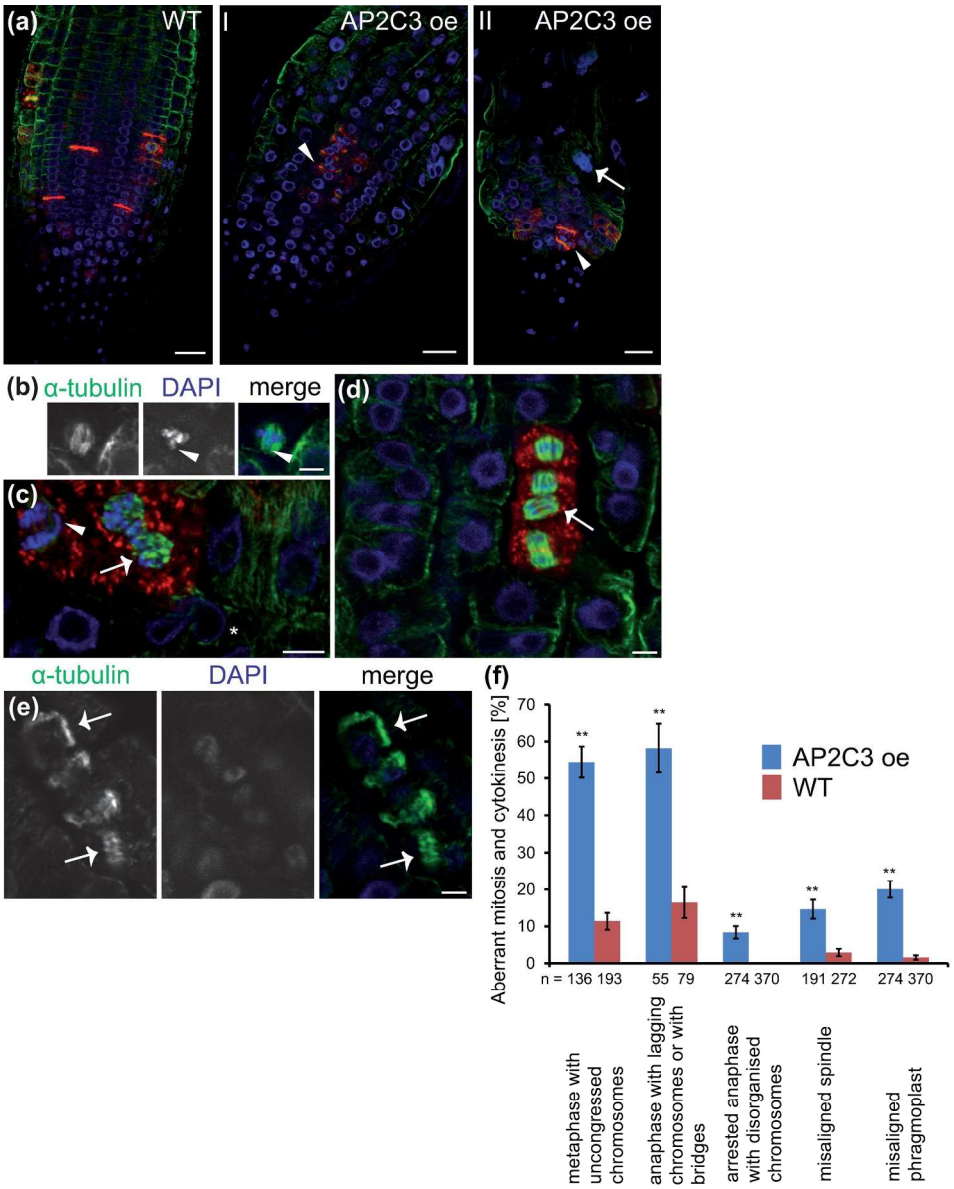

Fig7
197x244mm (300 x 300 DPI)

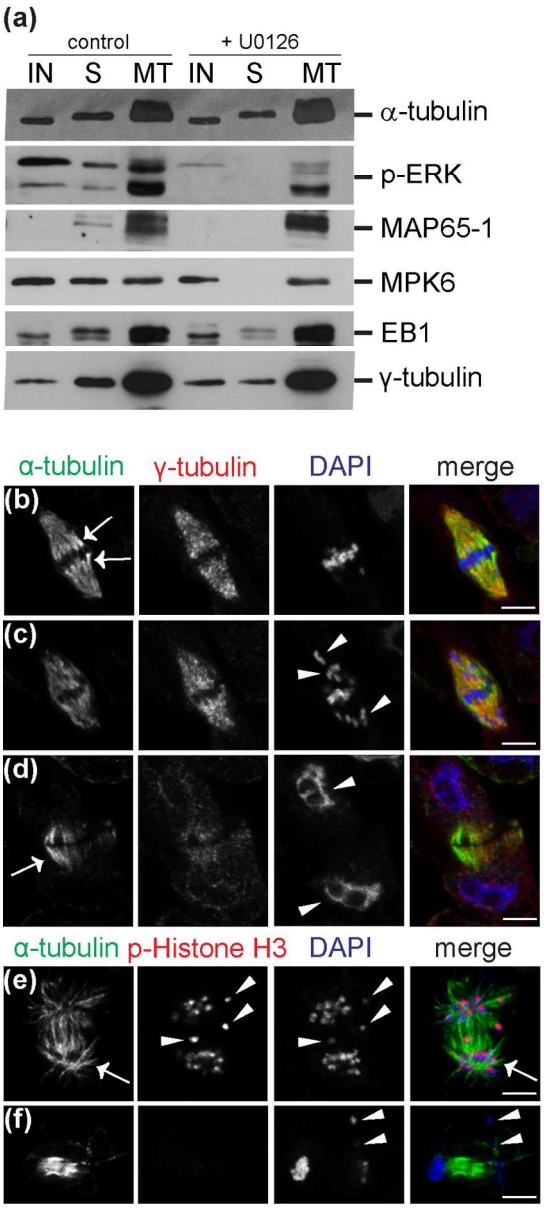

Fig8
83x184mm (300 x 300 DPI)